

# Non-paraxial Talbot Effect for Building Compact Spectrometers

Ningren Han<sup>1</sup>, Seong-Ho Cho<sup>1,2</sup>, Amir H. Atabaki<sup>1</sup>, Erika Ye<sup>1</sup>, William F. Herrington<sup>1</sup>,  
and Rajeev J. Ram<sup>1</sup>

<sup>1</sup>Massachusetts Institute of Technology, 77 Massachusetts Avenue, Cambridge, MA 02139, USA

<sup>2</sup>Samsung Advanced Institute of Technology, 130 Samsung-ro, Yeongtong-gu, Suwon-si, Gyeonggi-do, 443-803,  
Korea  
rajeev@mit.edu

**Abstract:** We explore the possibility of utilizing mid-field Talbot effect under non-paraxial diffraction for building compact spectrometers. Our experiment demonstrates nanometer resolution with a bandwidth over at least 100 nm for a Talbot spectrometer built using a standard 1-D transmission grating and a commercial CMOS imager. The effect of angular spread at the grating surface on spectral resolution is also investigated theoretically.

**OCIS codes:** 070.6760, 120.6200, 100.3190

## 1. Introduction

Computational spectrometers, either fiber/waveguide [1, 2] or free space-based [3, 4], emerge as interesting candidates for modern spectroscopy applications. As opposed to conventional grating-based spectrometers, these computational spectrometers do not require explicit orthogonal imaging in the far-field for wavelength distinction, but rather employ a non-orthogonal (but still invertible) wavelength dispersion mechanism with subsequent machine learning-like calibration and reconstruction processes. Examples of such dispersion mechanisms include 3-D photonic crystals [3], multimode fibers [2], and pseudo-random diffractive optics [4] among others. Because of the elimination of explicit orthogonal imaging optics, a computational approach opens possibilities for spectrometry with unconventional form factors as well as enhanced sensitivity due to the multiplexing advantage. Here, with a similar design principle in mind, we explore the possibility of utilizing the mid-field Talbot effect [5] under non-paraxial conditions as the dispersion mechanism for building a compact spectrometer.

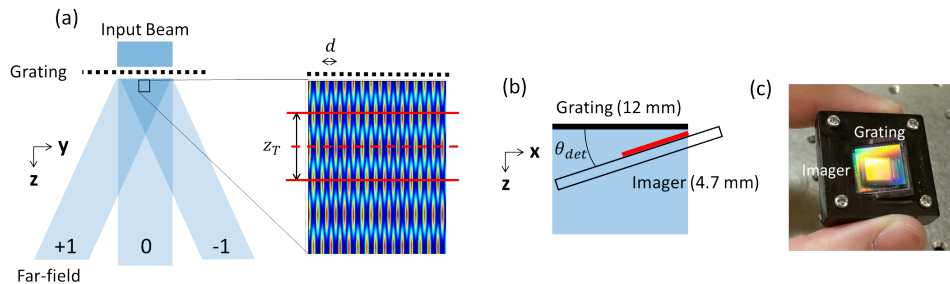


Fig. 1. (a) Illustration of the Talbot effect. (b) Schematic of the experimental setup for the tilted CMOS imager behind the 1-D grating. (c) Picture of the spectrometer.

## 2. Theory

The Talbot self-images occur when a spatially periodic object such as a transmission grating is illuminated by spatially coherent light. The self-image replicates itself along the direction perpendicular to the grating plane (the  $z$  direction) in an alternating phase-reversing fashion as shown in Figure 1 (a). In order to utilize the Talbot effect to build compact spectrometers, we constrain the Talbot self-images to be within a few millimeters behind the grating by choosing the grating pitch to operation under non-paraxial diffraction for the wavelengths of interest. The periodicity of the self-images  $z_T$  as a function of the wavelength  $\lambda$  in this case can be characterized as  $z_T(\lambda) = \lambda(1 - \sqrt{1 - \lambda^2/d^2})^{-1}$ , where  $d$  is the grating period. Assuming in the general case of arbitrary diffraction efficiencies of  $A_0$ ,  $A_1$  and  $A_{-1}$  for the three diffracted beams, the field intensity after the grating can be characterized as

$$I(x, z) \propto A_0^2 + A_1^2 + A_{-1}^2 + 2A_1A_{-1} \cos(4\pi x/d) + 2A_0(A_1 + A_{-1}) \cos(2\pi x/d) \cos(2\pi z/z_T) + 2A_0(A_1 - A_{-1}) \sin(2\pi x/d) \sin(2\pi z/z_T),$$

which is periodic in the  $z$  direction with the periodicity of  $z_T$  that determines the corresponding wavelength. A tilted CMOS imager is placed right behind the grating to sample the Talbot patterns across the  $z$  direction as shown in Figure 1 (b). The captured image can be subsequently transformed into spectrum of the source through standard Fourier transforms. The spectral resolution and maximum bandwidth without aliasing of the spectrometer can be determined by the total sampling length and spatial sampling period of the Talbot diffraction pattern, given by the projected sensor length and pixel size in the  $z$  direction due to the camera tilt  $\theta_{tilt}$ . Assuming that the sensor length is  $L$  and the pixel size is  $z_{pix}$ , the resolution  $\Delta k_T$  and bandwidth  $k_{T,max}$  in the spatial Fourier domain are determined as  $\Delta k_T = 2\pi(L \sin \theta_{tilt})^{-1}$  and  $k_{T,max} = \pi(z_{pix} \sin \theta_{tilt})^{-1}$ , where  $k_T = 2\pi/z_T$ . This provides a simple design guideline for a resolution and bandwidth target.

### 3. Experiment

To verify our model, we characterized spectrometers with off-the-shelf 1D transmission gratings and commercial CMOS imagers. With a size constraint in mind, we chose CMOS imagers for smartphone and compact camera applications, where the pixel size is at most a few micrometers. Our grating has a grating pitch of  $d = 1.035\mu m$  and our imager has a pixel size of  $z_{pix} = 1.12\mu m$ . The CMOS imager does not have any color filters, whereas the micro-lens array remains on top over the pixels. The glass protection window has been removed to prevent any spurious reflection. The imager has a dimension of  $4208 \times 3120$  pixels ( $4.713 \text{ mm} \times 3.494 \text{ mm}$ ), where the longer dimension is used to sample across the  $z$  direction to get a higher resolution. For characterizing our spectrometer, a tunable Ti:Sapphire laser in CW mode is coupled into a single mode fiber. The output of the fiber passes through a fiber collimation lens and a 10X beam expander. The collimated output beam is normally incident on the grating and the resulting Talbot pattern is recorded by the CMOS imager. For simplicity of characterization, the imager is placed to sample only the  $+1^{st}$  and the  $0^{th}$  order diffracted beams.

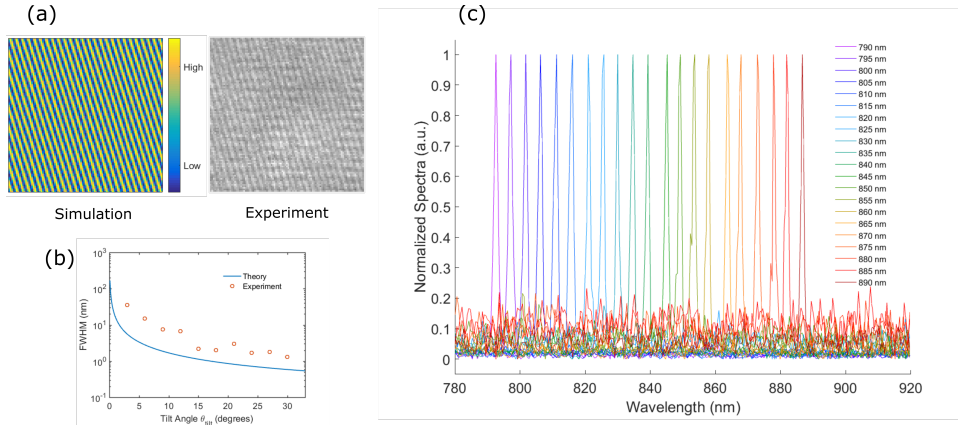


Fig. 2. (a) Simulated and captured Talbot pattern captured by the CMOS imager. (b) Measured spectral resolution as a function of tilt angle compared with the theory. (c) Transformed spectral peaks obtained from experiment with a tunable Ti:Sapphire laser across 100 nm.

Simulated and captured images for the sampled Talbot pattern are shown in Figure 2 (a) for an imager tilt angle of  $30^\circ$ . The periodic pattern of the self-images can be seen clearly from both images and the experiment agrees well with the simulation. To further verify our model of the Talbot spectrometer, the peak resolution, characterized as the full width at half maximum (FWHM) of the transformed spectral peaks, at 830 nm is plotted as a function of  $\theta_{det}$  in Figure 2 (b). A 10-row subsection of the full image is used for spectral reconstruction to avoid peak position variation across the image rows, possibly due to sampling distortion introduced by the presumed non-uniform displacement of the micro-lens array known as chief ray angle correction. As indicated in the figure, the resolution increases as the tilt angle increases as the theory predicts. At a tilt angle of  $30^\circ$ , a resolution close to 1 nm (1.3 nm) is achieved. A consistent resolution overestimation from the theory is observed across all the tilt angles, which could be attributed

to peak broadening due to pixel cross-talk for non-normal light incidence on the imager or the imager chief ray angle correction mentioned earlier. A series of transformed spectra across 100 nm from 790 to 890 nm at a tilt angle of  $30^\circ$  is plotted in Figure 3 (c), showing the wavelength dependency of the transformed spectral peaks.

#### 4. Discussions

Our experimental results suggest that the non-paraxial Talbot effect can be used as the dispersion mechanism for building a compact spectrometer with high resolution. A natural question that arises is how much spatial incoherence one can tolerate for a given resolution of such a spectrometer. We theoretically characterized the effective resolution with a given incidence angle spread over the polar and azimuthal directions on the grating for the Talbot spectrometer. Figure 3 (a) shows our simulation model, where the Talbot wave vector  $k_T$  arises due to the interference between the  $+1^{\text{st}}$  and  $-1^{\text{st}}$  order diffracted beams with the  $0^{\text{th}}$  order diffracted beam. An oblique incidence beam results in a shift in the Talbot wave vector  $k_T$  compared to the normal incidence case, and the shift depends on both  $\theta$  (in the  $x$ - $z$  plane) and  $\phi$  (in the  $y$ - $z$  plane). If the incidence beam has an angular spread, the ensemble of the shift effectively blurs  $k_T$  and reduces the resolution of the spectrometer. Due to the asymmetry of the wave vector deflection introduced by the grating, the effective resolution of the spectrometer suffers differently for  $\theta$  spread and  $\phi$  spread. In Figure 3 (c), we plot the theoretical effective resolution over incidence angle spread as a function of  $\theta$  spread and  $\phi$  spread under a  $30^\circ$  imager tilt, where the resolution under normal incidence is below 0.5 nm at  $\lambda = 830$  nm. The plot suggests that in order to maintain the resolution around one nanometer in this ideal model, one needs to restrain the angular spread  $\theta$  to be within around one degree and  $\phi$  to be within around one hundredths of a degree. This asymmetry of the dependence of effective resolution over  $\theta$  spread and  $\phi$  spread for the Talbot spectrometer is similar to that of a conventional spectrometer, where the spectrometer resolution is more sensitive over the width direction of the slit than the length direction of the slit due to the asymmetric dispersion from 1D gratings.

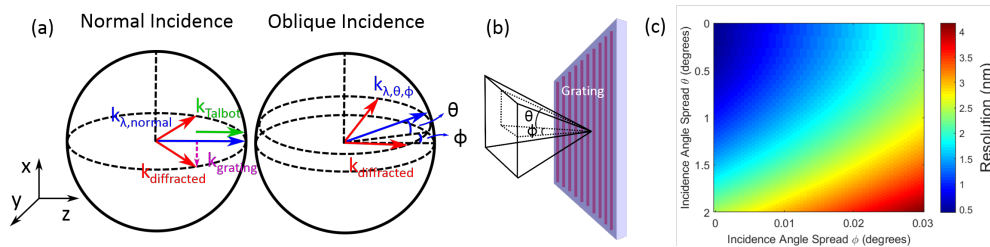


Fig. 3. (a) Wave vector scattering due to grating under normal and oblique incidence. (b) Illustration of the incidence angle spread on the grating surface used in calculating the plot in (c). (c) Effective resolution as a function of  $\theta$  spread and  $\phi$  spread for a camera tilt angle of  $30^\circ$ .

#### 5. Conclusions

In conclusion, our results demonstrate the potential of utilizing mid-field Talbot effect under non-paraxial diffraction for building compact spectrometers. Our model agrees well with experiment and can serve as a simple design guideline for constructing spectrometers with a given target performance metric.

#### References

1. B. Redding and H. Cao, "Using a multimode fiber as a high-resolution, low-loss spectrometer," *Optics letters* **37**, 3384–3386 (2012).
2. B. Redding, S. F. Liew, R. Sarma, and H. Cao, "Compact spectrometer based on a disordered photonic chip," *Nature Photonics* **7**, 746–751 (2013).
3. Z. Xu, Z. Wang, M. E. Sullivan, D. J. Brady, S. H. Foulger, and A. Adibi, "Multimodal multiplex spectroscopy using photonic crystals," *Optics express* **11**, 2126–2133 (2003).
4. P. Wang and R. Menon, "Computational spectrometer based on a broadband diffractive optic," *Optics express* **22**, 14,575–14,587 (2014).
5. H. L. Kung, A. Bhatnagar, and D. A. Miller, "Transform spectrometer based on measuring the periodicity of talbot self-images," *Optics letters* **26**, 1645–1647 (2001).